Emergent Materials
https://doi.org/10.1007/s42247-024-00840-9

ORIGINAL ARTICLE

Microfluidic vs. batch synthesis of fluorescent poly(GMA-co-EGDMA) micro/nanoparticles for biomedical applications

Betül Kılınçlı[1,2,3] · Ayşe Duru Çınar[4] · Barbaros Çetin[2,4] · Güneş Kibar[1,2,4]

Received: 6 June 2024 / Accepted: 11 August 2024

Abstract

Fluorescent particles play a crucial role in nanomedicine and biological applications such as imaging, diagnostic tools, drug delivery, biosensing, multimodal imaging, and theranostics. This report presents a novel synthesis method and comparative study for synthesizing fluorescent particles in microfluidic continuous and batch-type reactors. Glycidyl methacrylate (GMA) and ethylene glycol dimethyl acrylate (EGDMA) are well-known monomers for synthesizing functional particles for biomedical applications. Several methods exist to obtain fluorescent poly(GMA-co-EGDMA) (p(GMA-EGDMA)) particles through various polymerization techniques. Unlike existing methods, we developed a green approach for synthesizing fluorescent p(GMA-EGDMA) particles via UV-initiated one-step emulsion polymerization by comparing microfluidic and batch synthesis. Moreover, as a fluorescent dye, fluorescein isothiocyanate (FITC) was directly incorporated with p(GMA-EGDMA) particles at various concentrations to achieve tunable fluorescent functionality. While the batch synthesis resulted in polydisperse fluorescent p(GMA-EGDMA)microparticles with spherical shapes ranging from 25 µm to 1.0 µm in size, the microfluidic synthesis produced nonspherical nanoparticles. Fluorescent FITC@p(GMA-EGDMA) particles were characterized by scanning electron microscope (SEM), fluorescent microscope, and Fourier-transform infrared spectroscopy (FTIR). The synthesized particles have potential for fluorescence imaging applications, specifically biodetection in array systems.

Keywords Microparticles · Nanoparticles · UV-polymerization · Emulsion polymerization · Microreactors · Continuous synthesis · Green chemistry

1 Introduction

Fluorescent micro and nanoparticles have gained significant scientific attention in recent years due to their exceptional optical properties that glow by emitting light at a different wavelength after absorbing light [1]. These unique properties make them a viable option for a wide range of applications, including imaging [2], sensing [3] as well as drug delivery systems [4]. Unlocking the full potential of these applications hinges on the precise design of micro/nanoparticles with optimal size and functionality However, achieving this ideal size and functionality has always been a complex task, requiring careful consideration of multiple factors.

The synergy between fluorescent materials and polymer particles paves the way for developing a broad spectrum of fluorescent polymer micro/nanomaterials [5]. Among the various polymeric particles, poly(glycidyl methacrylate-co-ethylene glycol dimethyl acrylate) (p(GMA-EGDMA))

✉ Güneş Kibar
gkibar@atu.edu.tr

1 Micro Nano Particles (MNP) Research Group, Materials Science and Engineering Department, Adana Alparslan Turkes Science and Technology University, Adana 01250, Türkiye

2 UNAM—National Nanotech, Research Center and Institute of Materials Science & Nanotech, İ.D. Bilkent University, Ankara 06800, Türkiye

3 Food Engineering Department, Adana Alparslan Turkes Science and Technology University, Adana 01250, Türkiye

4 Microfluidics & Lab-on-a-chip Research Group, Mechanical Engineering Department, İ.D. Bilkent University, Ankara, Türkiye

Published online: 25 September 2024

stands out as a versatile material with extensive applications in both industrialand scientific fields [6]. Its popularity can be attributed to several favorable properties, including high reactivity of epoxy groups [7], cost-effectiveness [8], hydrophilicity [9], biocompatibility [10], and low cytotoxicity [11]. These properties make p(GMA-EGDMA) a valuable material for many applications, including chromatographic separation systems, drug delivery systems, dental implants, biosensors as well as catalyst carriers [12].

Many fluorescent dyes can be incorporated into methacrylate monomers (e.g., MMA, GMA, EGDMA, etc.) [5, 13]. The specific choice of fluorescent dye has a crucial role in designing the particle, as it significantly influences the emission properties of the resulting particles. Fluorescein isothiocyanate (FITC), one of the well-known fluorescent dyes, has been preferably employed for labeling biomolecules and nanoparticles [13]. The isothiocyanate group (-N = C = S) on FITC is highly reactive and can bond with primary amine groups. However, incorporating FITC into fluorescent particles requires specific considerations during synthesis to ensure optimal performance. The covalent binding of the dye to the particle is crucial for imaging and tracking in experimental studies to prevent dye dissociation and leaching [14]. Currently, a series of synthesis methods have been available in the literature to synthesize or fabricate fluorescent micro- and nanoparticles, including various polymerization techniques such as emulsion [15], suspension [16], precipitation [17], and dispersion polymerization [18]), hydro/solvothermal method [19], sol-gel method [20], and post modification techniques on particles [21]. Within these methods, one-step emulsion polymerization has been preferably implemented to synthesize functional polymeric particles due to its simplicity over multi-step processes.

Beyond traditional batch synthesis techniques, microfluidic techniques enabled the continuous synthesis of polymeric particles, offering various design features such as multiple channels and variable lengths [22]. Microfluidic reactors provide a novel alternative to batch-type reactors for obtaining polymeric micro/nanoparticles by allowing precise control over differential volumes using various synthesis methods, including continuous flow [23], droplet generation [24], flow-focusing [25], and precipitation [26].

There were efforts to obtain p(GMA-EGDMA) particles in the literature through batch or microfluidic methods. Gokmen et al. [27] synthesized classical porous p(GMA-EGDMA) microparticles in a microfluidic reactor through one-step emulsion polymerization, preparing a monomer phase in cyclohexanol and dodecanol. Even though the particles were uniformly synthesized in a one-step emulsion, the emulsion consisted of toxic solvents such as cyclohexanol with no-fluorescent character. Similarly, another study synthesized p(GMA-EGDMA) microparticles in a batch system using one-step emulsion polymerization with a monomer phase prepared in toluene and decan-1-ol [28]. That study showed that batch synthesis methods were applicable to obtain p(GMA-EGDMA) microparticles; however, the synthesis procedure contained some toxic solvents such as toluene and THF, and the resultant product had no fluorescent activity. Alternatively, p(GMA-EGDMA) microparticles (ca. 160 µm in size) were also obtained in one-step UV-polymerization using a tubing-needle-based microfluidic setup for mixing SDS water phase and monomer-porogen containing discrete phase [29]. In the same study, p(GMA-EGDMA) microparticles had a second treatment with amine-functionalized fluorescent inks to fabricate Janus particles *via* microcontact printing methodology. The fluorescent p(GMA-EGDMA) particles were also synthesized together with N-vinyl carbazole (NVCz: a conductive and photo-dependent monomer) *via* thermally initiated distillation-precipitation polymerization using acetonitrile during the distillation process [30]. Although the distillation-precipitation polymerization method allowed fabricating p(GMA-EGDMA) shell particles with fluorescent NVCz molecule in the chemical structure, the method had some steps, and each step was at least 30 min with a total 4 h synthesis protocol. Briefly, these methods require toxic organic solvents or some steps to obtain fluorescent p(GMA-EGDMA) particles.

In this study, unlike existing methods, we present a green approach for synthesizing fluorescent p(GMA-EGDMA) *via* one-step emulsion polymerization. Green synthesis techniques have gained prominence in recent years for the production of micro/nanoparticles due to their use of non-toxic, sustainable, and environmentally friendly materials and conditions [31–33]. Our study aimed to replace toxic solvents (e.g., toluene, acetonitrile, etc.) with ethanol and develop a one-step UV-initiated emulsion polymerization through free radical mechanisms. Another aspect of this study was the incorporation of the fluorescent dye FITC, polymerized with methacrylate monomers in various concentrations to achieve tunable fluorescent functionality. Additionally, the effect of the reactor type was examined by comparing microfluidic and batch synthesis methods for all different concentrations. The fluorescent p(GMA-EGDMA) particles were characterized using SEM, EDAX, fluorescence microscopy, and FTIR. The obtained particles could be promising for fluorescence imaging applications, specifically bio-detection in array systems.

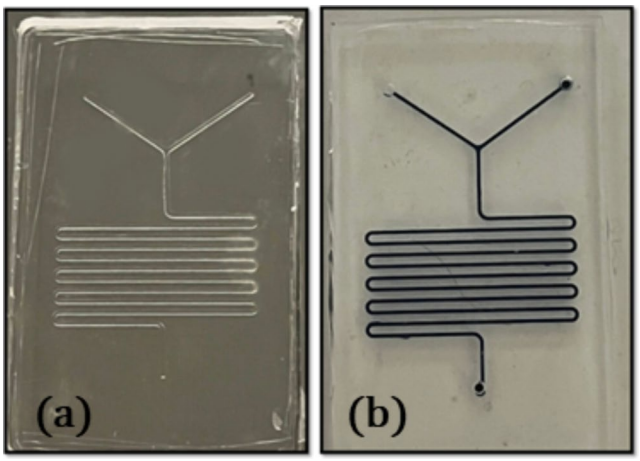

Fig. 1 The microfluidic reactor fabrication **(a)** plastic mold containing microchannel geometry 400 µm × 400 µm (height and width) **(b)** PDMS microfluidic reactor 50 mm × 30 mm (height and width)

2 Experimental

2.1 Materials and methods

The epoxy-functional monomer glycidyl methacrylate (GMA) and the crosslinking agent ethylene glycol dimethyl acrylate (EGDMA) were procured from Sigma-Aldrich. Additional reagents including the emulsifying agent sodium dodecyl sulfate (SDS), the fluorescent dye fluorescein isothiocyanate (FITC), and the photoinitiator 2-hydroxy-2-methylpropiophenone (Darocur 1173 or HMPP) were also sourced from Sigma-Aldrich. The polydimethylsiloxane (PDMS) SYLGARD 184 silicone elastomer kit was obtained from Dow Corning GmbH, Germany. Solvents such as ethanol and acetone were purchased from Merck. Deionized water (dH_2O) used in all experiments was obtained using a Millipore Direct-Q 3UV water purification system.

2.2 Fabrication of the microfluidic reactor

The fabrication of molds with micro-features is crucial, as it directly affects the quality of the microchannels in microfluidic devices. This process requires the design of the microchannel network and the corresponding mold design using CAD software, preparation of the computer-aided manufacturing (CAM) program, and careful execution of the machining process. The microfluidic reactor was designed with two inlets and one outlet to allow continuous flow during the particle synthesis process in Fig. 1. During the development of the CAM program, adaptive feed rate control options and interpass cleaning strategies were employed. High-precision milling operations were performed on a DECKEL MAHO-HSC55 milling center, which was equipped with an NSK HES510-HSKA63 high-speed spindle featuring a runout of less than one micrometer at the Bilkent University Micro System Design and Manufacturing Center. The mold was fabricated out of plexiglas to obtain microchannels with channel dimensions of 400 µm × 400 µm (height and width) (Fig. 1a) [34, 35].

2.3 Synthesis of fluorescent p(GMA-EGDMA) particles

The fluorescent p(GMA-EGDMA) particles were obtained through one-step emulsion polymerization. The pre-emulsion solutions contained monomers (GMA and EGDMA), surfactant (SDS), fluorescent dye (FITC), UV initiator (Darocur 1173), and solvents (water and ethanol) with a certain amount (Table 1). The pre-emulsions were prepared by adding the organic phase into the water phase, then emulsified for 5 min in an ultrasonic bath (KUDOS Ultrasonic Cleaner, Shanghai, China). Increasing FITC concentrations changed the pre-emulsion color from white to yellowish (Fig. 2a-top image). Under UV irradiation, the pre-emulsion solutions exhibited a gradient in fluorescent intensity, appearing as increasingly bright green colors (Fig. 2a-bottom image). The prepared pre-emulsion solutions (without

Table 1 The one-step UV curable emulsion mixture of varying FITC stock solution amounts

Components	Particle nomenclature					
	F0	F1	F10	F25	F50	F100
Organic phase						
GMA	0.250µL	0.250µL	0.250µL	0.250µL	0.250µL	0.250µL
EGDMA	0.250µL	0.250µL	0.250µL	0.250µL	0.250µL	0.250µL
Darocur1173	40µL	40µL	40µL	40µL	40µL	40µL
Ethanol	500µL	495µL	450µL	375µL	250µL	-
FITC stock*	-	5µL	50µL	125µL	250µL	500µL
Water phase						
SDS	12.5 mg	12.5 mg	12.5 mg	12.5 mg	12.5 mg	12.5 mg
Water	5mL	5mL	5mL	5mL	5mL	5mL

* The FITC stock solution was prepared as 0.5 mg/mL in ethanol

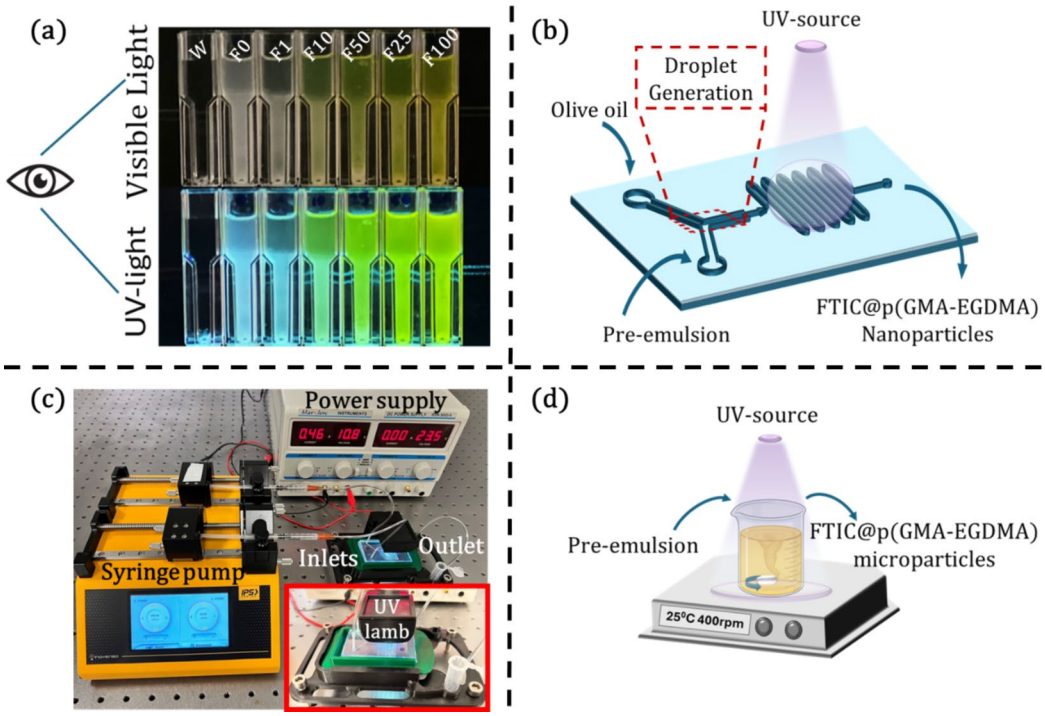

Fig. 2 **(a)** Photographs of fluorescent p(GMA-EGDMA) pre-emulsion in varying FITC concentrations under different UV irradiation conditions top image: without UV exposure and bottom image: under UV-exposure (W: water, nomenclature was from Table 1), the representative figures of synthesis of fluorescent P(GMA-EGDMA) **(b)** microfluidic synthesis, **(c)** batch-type, and **(d)** the experimental set-up for microfluidic reactor

UV exposure) were divided into two portions in volume for batch and microfluidic synthesis via UV polymerization.

2.3.1 Microfluidic synthesis

The pre-emulsion mixtures (Table 1) were transferred into a plastic syringe and introduced into a microfluidic reactor via one inlet (Fig. 2b). Olive oil was similarly loaded into a plastic syringe and connected to the microfluidic reactor through another inlet (Fig. 2b). Initially, the microchannels were filled with oil at a flow rate of 50 µL/min. Subsequently, the pre-emulsion was introduced into the microchannels at a flow rate of 100 µL/min using a syringe pump (IPS 14R, Inovenso Ltd, Türkiye). Upon formation of the droplets, a UV lamp was positioned above the microfluidic reactor and activated to initiate the free radical UV polymerization (Fig. 2c). The washing step of the microchannels with oil was critical to prevent clogging during the reaction. The resulting FITC@p(GMA-EGDMA) particles were collected in an Eppendorf tube. The reaction medium and oil were removed through centrifugation, followed by successive washing steps with acetone, ethanol, and water. The FITC@p(GMA-EGDMA) particles were kept at 4 °C in the dark for further analysis.

2.3.2 Batch synthesis

The pre-emulsion mixtures (Table 1) were transferred into a plastic beaker and mixed with a magnetic stirrer at 400 rpm at room temperature. The UV source (10 W High Power Led UV Chip − 365 nm) initiated the free radical polymerization. The UV source was placed over the magnetic stirrer system (Fig. 2d) and exposed for 5 min to complete the reaction. After the reaction, the FITC@p(GMA-EGDMA) particles were obtained and collected via centrifugation. The reaction medium and unreacted substances were removed in subsequent washing steps with ethanol and water. The FITC@p(GMA-EGDMA) particles were kept at 4 °C in the dark for further analysis.

2.4 Characterization of fluorescent p(GMA-EGDMA) particles

The morphological properties of fluorescent p(GMA-EGDMA) particles were characterized using scanning electron microscopy (SEM) (Quanta 450, Akishima, Tokyo, Japan). For sample preparation, the particles were dispersed in ethanol using a vortex mixer. Subsequently, 5 µL of the particle solution was deposited onto double-sided adhesive carbon tapes affixed to a flat sample holder and allowed to air-dry for 5 min. To ensure a conductive surface and to

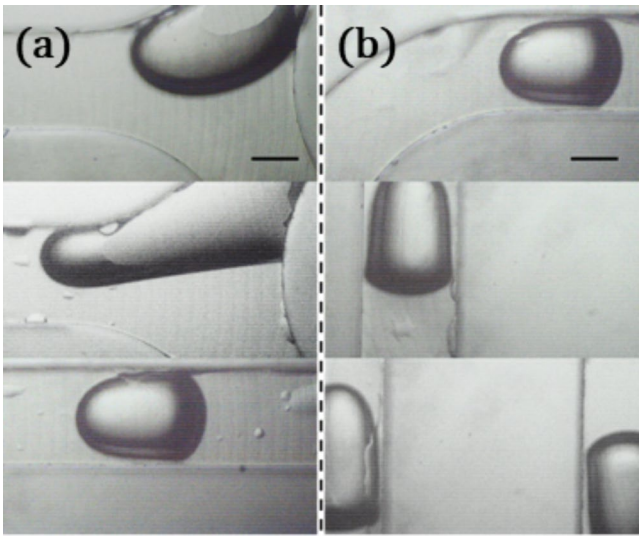

Fig. 3 Microscope images of **(a)** the droplet generation part and **(b)** the UV-irradiation part in the microfluidic reactor. The microscope images were captured at a flow rate ten times slower than the experimental conditions, using an inverted microscope (PSARON-FluidoScope) at 4x magnification with 200 µm bar

protect the particles from thermal degradation during SEM analysis, the samples were coated with a 6 nm Au–Pt thin film. The size distribution of synthesized particles was analyzed via Mastersizer Hybrid (Malvern, UK) and Zetasizer Nano ZS (Malvern, UK). The fluorescent characters were analyzed via fluorescent and differential interference contrast (DIC) microscope-upright (Zeiss Axio Scope A1, Germany). Brightfield and fluorescent images were taken of each particle under constant exposure. A UV source (20% power) was used during the fluorescent image with a 500ms exposure time and 30% intensity. Additionally, the fluorescence intensity of reaction medium was measured before and after the reaction using FLUOstar Omega Microplate Reader. The chemical structure of the particles was determined by Fourier-transform infrared spectroscopy FTIR (Thermo Scientific Nicolet™, USA). FTIR spectrums were collected for the powder form of particles and liquid form of monomers by scanning between 4000 and 500 cm^{-1}.

3 Results and discussion

The fluorescent p(GMA-EGDMA) were synthesized via UV-polymerization form pre-emulsion using one-step batch and microfluidic synthesis methods. Half of the pre-emulsion flowed through the microfluidic reactor. The pre-emulsion droplets were generated in the Y junction (Fig. 3a). The GMA-EGDMA pre-emulsion droplets passed through the UV-irradiation section of the chip. The continuous flow of oil provided a steady progression and prevented clogging of the microchannels during the UV-polymerization of fluorescent p(GMA-EGDMA) particles (Fig. 3b).

The morphological character of fluorescent p(GMA-EGDMA) particles was determined via SEM images (Fig. 4). Although some microparticles were also observed as a resultant product in the microfluidic system (not shown in SEM images), the overall morphological characteristics of the fluorescent p(GMA-EGDMA) were predominantly in the form of nanoparticles (Fig. 4-top panel). While fluorescent p(GMA-EGDMA) nanoparticles were formed using

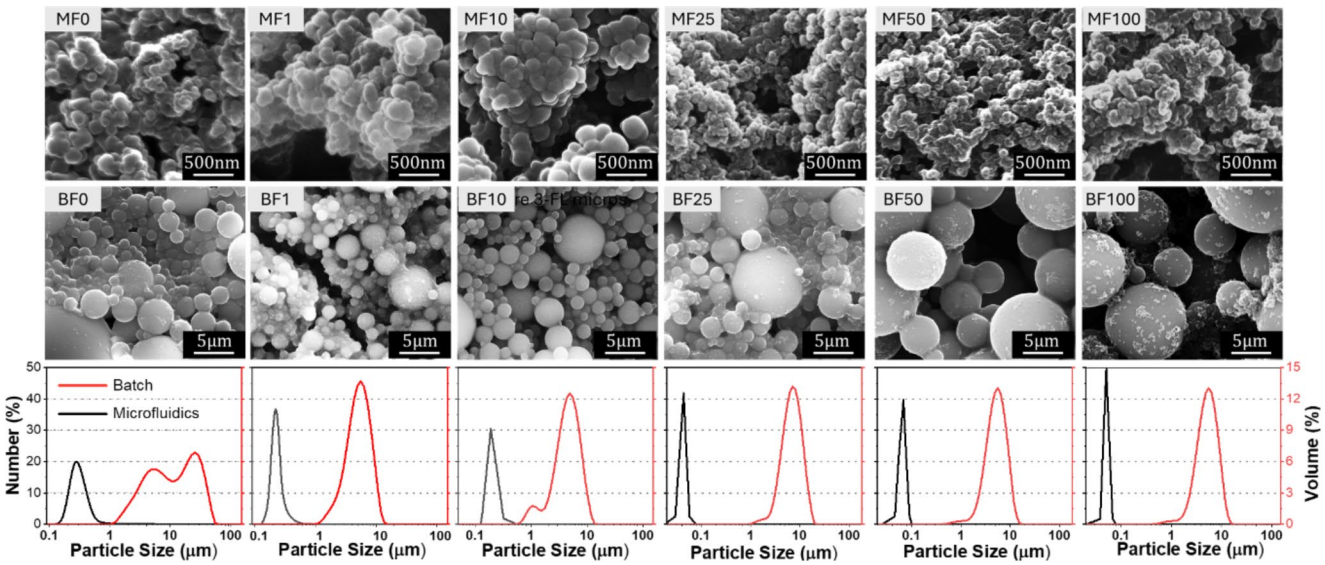

Fig. 4 SEM images of fluorescent p(GMA-EGDMA) particles **(top panel)** microfluidic-type reactor synthesis "M" denoted microfluidic synthesis results of different FITC concentrations (SEM images at 10000X and 100000X magnification with 5 µm and 500 nm scale bars, respectively), and **(bottom panel)** batch-type reactor synthesis "B" denoted the batch synthesis, the particle size distribution were given as number(%) for microfluidic-synthesized in black color, volume (%) for batch-synthesized in red color

the microfluidic reactor, spherical particles were obtained using the batch system (Fig. 4-bottom panel). The batch-type reactor synthesis produced spherical fluorescent p(GMA-EGDMA) microparticles with a polydisperse size distribution ranging from 1 μm to 25 μm. The dynamic light scattering (DLS) analysis was performed to address this size difference. The particle size distribution was characterized as number (%) for microfluidically synthesized particles and volume (%) for batch-synthesized particles. These results have been incorporated alongside SEM data. Our findings indicate that the microfluidically synthesized particles exhibit a narrow size distribution in the nanoscale range, whereas the batch-synthesized particles display a polydisperse size distribution in the micron range.

The hydrodynamic size and polydispersity of the prepared particles were influenced by several critical parameters such as mixing conditions and solvent composition. The intensity and method of mixing play a significant role in determining the size distribution and polydispersity of particles. Efficient mixing ensures uniform distribution of solutes and solvents [36]. The effectiveness of mixing significantly influenced the morphological characteristics of the resultant product. In the batch-wise reactor system, the pre-emulsion was magnetically stirred. This mixing environment led to the formation of polydisperse micelles of the surfactant, containing organic phase (monomers, a UV initiator, and a fluorophore molecule). Upon exposure to UV irradiation, these micelles in pre-emulsion rapidly formed FITC@p(GMA-EGDMA) microparticles. On the other hand, the same pre-emulsion solution resulted in the formation of nanoparticles in a microfluidic reactor system.

During microfluidic synthesis, the organic phase was dispersed in small volumes of water-surfactant droplets. Unlike large-volume batch-type reactors with magnetic stirring, the micelles in the microfluidic system were mixed within microliter-volume droplets flowing through microchannels. This micro-volume mixing environment could likely contribute to a reduction in micelle size. In addition, the choice and ratio of solvents were crucial in controlling the hydrodynamic size and polydispersity of particles. The miscibility between the organic and the water phases (the ethanol-water solvent system) could also account for this size reduction. The homogeneous organic phase was prepared by dissolving all the organic molecules —GMA, EGDMA, Darocur, and FITC—in ethanol. FITCis a fluorescent dye commonly employed in biological research. Its solubility is in various solvents, such as dimethyl sulfoxide (DMSO), ethanol, and dimethylformamide (DMF) (Bu cümle kontrol edilsin). GMA is an epoxy-functional monomer with moderate polarity. The solubility of FITC in GMA may be limited due to the polar and reactive nature of GMA. EGDMA is a cross-linking agent with two methacrylate groups and is less polar compared to GMA. The solubility of FITC in EGDMA may also be limited, as EGDMA is not as polar as the solvents in which FITC is usually dissolved effectively. That is why, ethanol was selected as the non-toxic organic solvent to prepare the pre-emulsion due to the high solubility of fluorophore molecule FITC. Although ethanol is miscible with many organic solvents, it also has the unique ability to dissolve in water. Therefore, ethanol could penetrate the water medium, decrease the interfacial tension, and reduce the size of the micelles [37]. Thus, the micro-mixing process in small-volume droplets, coupled with the properties of ethanol, played a crucial role in producing nanoparticles by reducing micelle size to form nanoparticles.

The fluorescent microscope images of p(GMA-EGDMA) particles showed differences in fluorescence intensity throughout photos displaying a gradient of FITC concentrations (Fig. 5) irrespective of the synthesis method employed—batch or microfluidic. The highest concentration of FITC (0.5 mg/mL, denoted as F100) notably exhibited the ultrabright character within the images. However, the luminosity observed in the images gradually diminished as the FITC concentration decreased. In particular, particles synthesized with a FITC concentration of 0.05 mg/mL (denoted as F10) retained slightly detectable brightness under consistent UV exposure. Beyond this threshold, the insufficient amount of FITC resulted in diminished fluorescence within the microscope images.

Furthermore, the incorporation of FITC could be observed on particles in Fig. 5. FITC was distributed throughout both the core and the shell of the polymer particles. This uniform fluorescence across the entire particle suggested that FITC molecules were not confined to a specific region but are rather well-dispersed within the particle matrix. This homogeneous distribution was indicative of an effective encapsulation process during particle synthesis. The process of incorporating FITC into the poly(GMA-co-EGDMA) particles likely involved several key mechanisms, such as the copolymerization process and solvent effects. During the synthesis of poly(GMA-co-EGDMA) particles, FITC can be co-polymerized with GMA and EGDMA. The isothiocyanate group of FITC could react with the epoxy groups of GMA, leading to the covalent attachment of FITC within the polymer network. This chemical incorporation provided that FITC was distributed uniformly throughout the polymer matrix.

The selection of solvent (ethanol) during the particle formation process may influence the solubility and distribution of FITC. In a well-mixed system, FITC could be evenly dispersed in the monomer solution before polymerization, resulting in uniform distribution within the formed particles. To investigate this, we measured the amount of FITC in the reaction medium using fluorescence intensity before

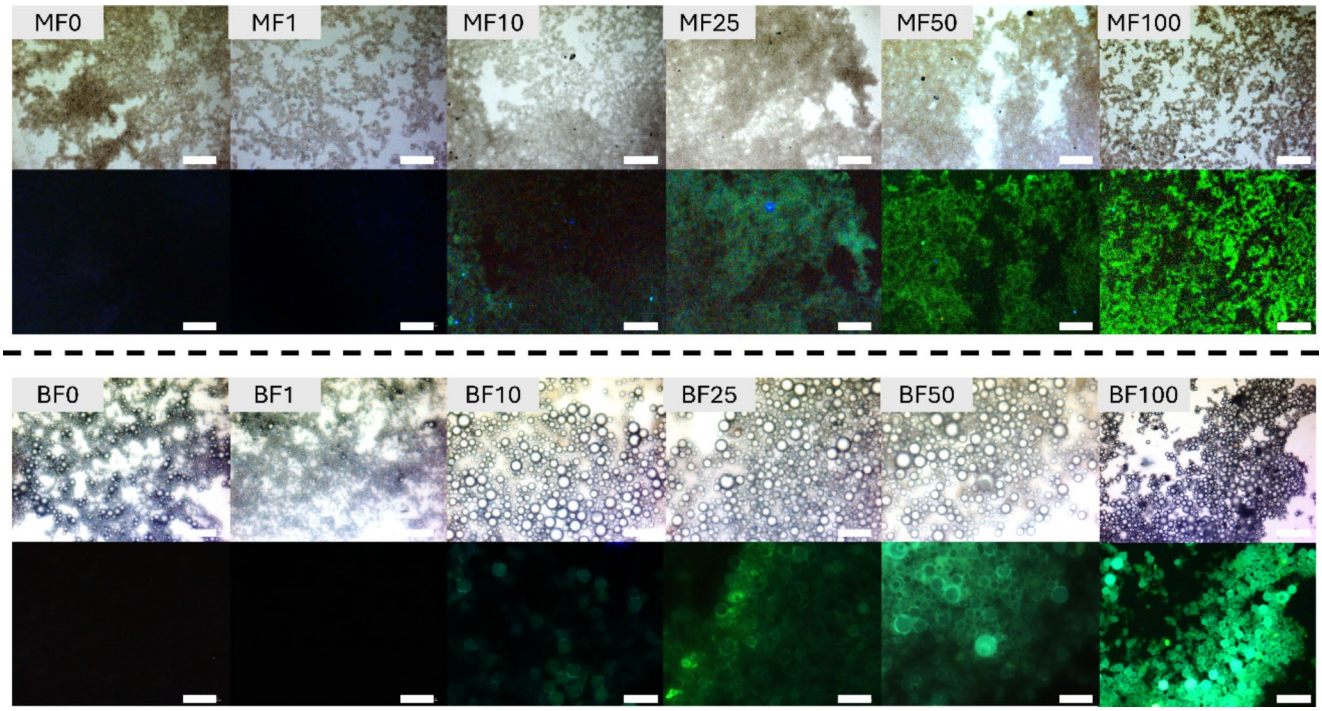

Fig. 5 The fluorescent microscope images of FTIC@p(GMA-EGDMA) micro/nanoparticles synthesized in **(top panel)** microfluidic reactor "M" denoted microfluidic synthesis results of different FITC concentrations and **(bottom panel)** batch-type reactor "B" denoted the batch synthesis (scale bar represents 50 μm)

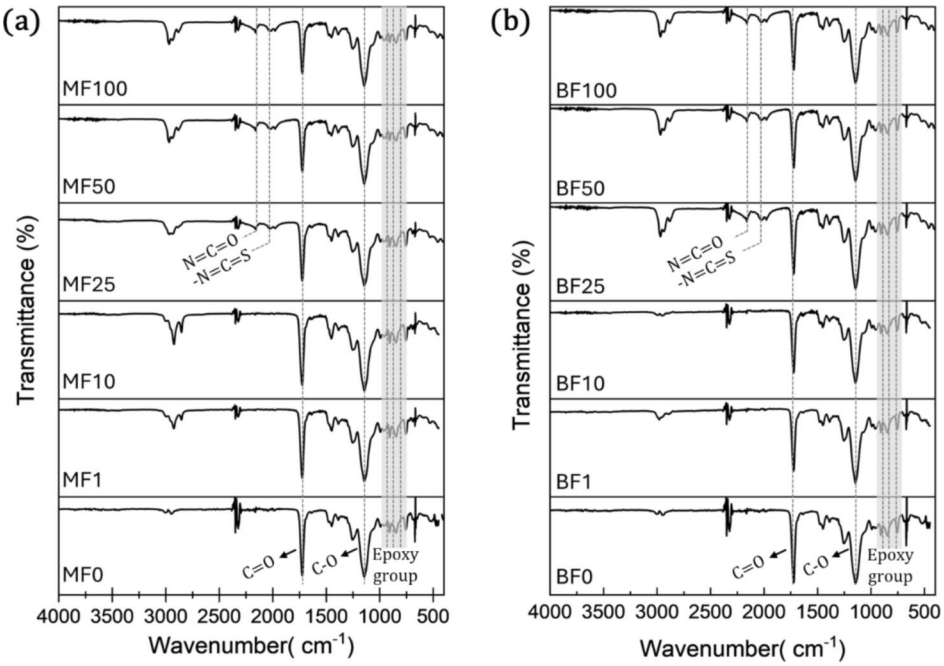

Fig. 6 FTIR spectra of p(GMA-EGDMA) particles synthesized with different FITC concentrations in **(a)** microfluidic reactor "M" denoted microfluidic synthesis and **(b)** batch-type reactor "B" denoted the batch synthesis

polymerization. Furthermore, we quantified the amount of FITC remaining in the supernatant after the reaction. Our results indicated a significant decrease in the FITC concentration in the supernatant after the reaction, suggesting that the majority of FITC (> 94.5%) was successfully incorporated into the particles (please see Figure S1 and Table S1 in the supp. info).

The chemical structure of FITC@p(GMA-EGDMA) micro/nanoparticles was determined via FTIR analysis (Fig. 6). The batch and microfluidic synthesis of p(GMA-EGDMA) particles resulted in a similar chemical

structure for each FITC concentration. The FITC presence in the chemical composition was evident through peaks at 1980 cm^{-1}, 2015 cm^{-1}, and 2160 $cm^{-1,}$ representing isothiocyanate (-N=C=S) groups and isocyanate groups (N=C=O) stretching vibration in the spectral analysis of particles denoted as F25, F50, and F100, regardless of whether a microfluidic or batch synthesis approach was utilized (Fig. 6a and b) [38]. These bonds ensured the stability and retention of the dye on the particle, thereby enhancing the accuracy and reliability of imaging data. Such stability is essential in complex experimental environments, where non-covalent interactions may lead to dye dissociation and consequent signal loss, undermining the fidelity of the tracking and imaging processes [39]. The peak observed at approximately 1720 cm^{-1} signified the presence of carbonyl groups (-C=O-) bonds within the methacrylate monomers [40, 41]. Additionally, the epoxy ring functionality of GMA was observed with asymmetric vibration peaks around 757, 845, and 910 cm^{-1} for all synthesized p(GMA-EGDMA) particles (Fig. 6a and b) [42, 43]. The strong peak at 1145 cm^{-1} was associated with the stretching vibrations of the ester (C–O) group within the chemical structure [44]. Specifically, the active vinyl end group -C=C- of GMA and EGDMA monomers (please see Figure S2 in the supp. info) were not observed around 1640 cm^{-1} in synthesized particles FTIR spectra (Fig. 6a and b) [40, 41]. The absence of the methacrylate double bond indicates the successful completion of the free radical polymerization mechanism via one-step UV-initiated emulsion polymerization for both the microfluidic and batch synthesis methods.

4 Concluding remarks

Fluorescent micro/nano particles have consistently captivated researchers because of their wide range of potential uses across different fields. Here, we present a novel one-step green approach for synthesizing fluorescent p(GMA-EGDMA) particles, contrasting outcomes between batch and microfluidic reactor-based synthesis. Both synthesis methods successfully yielded the fluorescent p(GMA-EGDMA) particles via one-step UV-initiated emulsion polymerization through free radical mechanisms. However, batch synthesis offers advantages in accessibility, ease of handling, and the rapid completion of polymerization within a short timeframe (e.g., 5 min) in comparison to microfluidic synthesis. In addition, the characterization of the synthesized particles revealed significant morphological differences between the two synthesis methods. The batch synthesis resulted in polydisperse microparticles, whereas the microfluidic synthesis predominantly produced nanoparticles, showcasing the influence of the mixing environment on particle morphology. By optimizing mixing conditions and solvent composition, in the future studies it is possible to fine-tune the hydrodynamic size and polydispersity of the particles to meet specific requirements. Fluorescence microscopy, spectroscopy and FTIR analysis confirmed the presence of fluorescent dye FITC within the chemical structure of the particles, validating their potential for fluorescent imaging applications. Moreover, the stability of FITC on the particles was demonstrated, ensuring reliable imaging data acquisition. Additionally, the presence of epoxy functionality in the chemical structure of fluorescent particles enables further modifications. Therefore, the fluorescent p(GMA-EGDMA) particles emerge as highly promising materials for various applications. Spherical micro/nanoparticles may have the potential to be utilized in biosensors [45], chromatographic separations [46], or novel isolation/detection systems [47], while nonspherical ones may exhibit great potential for specific applications like receptor-mediated endocytosis and phagocytosis due to their unique curvature and greater surface area [48, 49].

As a future research direction, the pre-emulsion could be modified with different methacrylate monomers, surfactants, and solvents to examine the effects on the resultant product as size distribution, colloidal stability, and functional properties for both synthesis methods. For example, the impact of different surfactants and amounts may be investigated. Surfactants such as sodium dodecyl sulfate (SDS, negatively charged), cetyltrimethylammonium bromide (CTAB, positively charged), and non-ionic surfactants like Tween-20 may be utilized to modify the surface properties of the particles and enhance their stability. Despite the appeal of microfluidic synthesis for its ability to produce results in micro volumes, there is still room for improvement of the microfluidic reaction to overcome its limitations and capitalize on its potential benefits. Addressing the issue of pre-emulsion loss in tubing may be crucial for advancing the microfluidic reactor. Furthermore, introducing innovative systems, such as a flexible hydraulic reservoir (FHR), may hold promise for reducing reagent consumption, enhancing efficiency, and minimizing waste [50, 51].

Supplementary Information The online version contains supplementary material available at https://doi.org/10.1007/s42247-024-00840-9.

Acknowledgements Dr. G. Kibar would like to thank the financial support from the Scientific and Technological Research Council of Türkiye (TÜBİTAK-2218, Award Grand No.: 122C228) and Adana Alparslan Türkeş Science and Technology University (Scientific Research Project, Grant No. 22103005). B. Kılınçlı also acknowledges the financial support provided by TÜBİTAK through the BİÇABA Program. A.D. Çınar extends gratitude to the Intern Researcher Scholarship Program (TÜBİTAK 2247-C STAR 2023/2) for their support. The authors give special thanks to Toprak Karaman for the 3D-printed platform for the experimental microfluidic synthesis setup and Reyhan Sever for preparing the mold photos of the microfluidic reactor.

Data availability All data collected, generated, or analyzed during the study are included in this published article and its supplementary information files.

Declarations

Competing interests None.

References

1. R. Mahato, *Multifunctional micro-and Nanoparticles. Emerging Nanotechnologies for Diagnostics, drug Delivery and Medical Devices* (Elsevier, 2017), pp. 21–43
2. J. Caldwell, R. Lehner, S. Balog, C. Rhême, X. Gao, D. Septiadi et al., Fluorescent plastic nanoparticles to track their interaction and fate in physiological environments. Environ. Science: Nano. **8**(2), 502–513 (2021)
3. C. Kromer, K. Schwibbert, A.K. Gadicherla, D. Thiele, N. Nirmalananthan-Budau, P. Laux et al., Monitoring and imaging pH in biofilms utilizing a fluorescent polymeric nanosensor. Sci. Rep. **12**(1), 9823 (2022)
4. N. Kapate, J.R. Clegg, S. Mitragotri, Non-spherical micro-and nanoparticles for drug delivery: progress over 15 years. Adv. Drug Deliv. Rev. **177**, 113807 (2021)
5. H. Zhong, B. Zhao, J. Deng, Synthesis and application of fluorescent polymer micro-and nanoparticles. Small. **19**(26), 2300961 (2023)
6. E.B. Simsek, D. Saloglu, A.A. Aydın, Investigation of adsorption and biosorption features of bio-functionalized poly (GMA-Co-EGDMA) polymer beads in the treatment of nicotine from tobacco industry. Environ. Sci. Pollut. Res. **30**(24), 65801–65821 (2023)
7. R.V. Hercigonja, D.D. Maksin, A.B. Nastasović, S.S. Trifunović, P.B. Glodić, A.E. Onjia, Adsorptive removal of technetium-99 using macroporous poly (GMA-co-EGDMA) modified with diethylene triamine. J. Appl. Polym. Sci. **123**(2), 1273–1282 (2012)
8. G. Flores-Rojas, E. Bucio, Radiation-grafting of ethylene glycol dimethacrylate (EGDMA) and glycidyl methacrylate (GMA) onto silicone rubber. Radiat. Phys. Chem. **127**, 21–26 (2016)
9. G. Chen, R. Chen, C. Zou, D. Yang, Z.-S. Chen, Fragmented polymer nanotubes from sonication-induced scission with a thermo-responsive gating system for anti-cancer drug delivery. J. Mater. Chem. B **2**(10), 1327–1334 (2014)
10. T. Anirudhan, V. Manjusha, V.C. Sekhar, A new biodegradable nano cellulose-based drug delivery system for pH-controlled delivery of curcumin. Int. J. Biol. Macromol. **183**, 2044–2054 (2021)
11. J. Hernandez, A. Robb, S. Servera, N. Bedrosian, O. Gomez, Z. Duca et al., Synthesis and characterization of Amorphous Lawsone Polymer dots for fluorescent applications. ACS Appl. Nano Mater. **6**(22), 20639–20651 (2023)
12. J. Xiao, Q. Lu, H. Cong, Y. Shen, B. Yu, Microporous poly (glycidyl methacrylate-co-ethylene glycol dimethyl acrylate) microspheres: synthesis, functionalization and applications. Polym. Chem. **12**(42), 6050–6070 (2021)
13. M.-J. Zhang, W. Wang, X.-L. Yang, B. Ma, Y.-M. Liu, R. Xie et al., Uniform microparticles with controllable highly interconnected hierarchical porous structures. ACS Appl. Mater. Interfaces. **7**(25), 13758–13767 (2015)
14. V. Zhukova, N. Osipova, A. Semyonkin, J. Malinovskaya, P. Melnikov, M. Valikhov et al., Fluorescently labeled plga nanoparticles for visualization in vitro and in vivo: the importance of dye properties. Pharmaceutics. **13**(8), 1145 (2021)
15. P. Kasaei, N. Karami, J.K. Rad, S. Sanjabi, A.R. Mahdavian, Modified cellulose paper with photoluminescent acrylic copolymer nanoparticles containing fluorescein as pH-sensitive indicator. Carbohydr. Polym. **296**, 119965 (2022)
16. H. Yang, L. Hu, C. Chen, H. Zhao, P. Wang, T. Zhu et al., Influence mechanism of fluorescent monomer on the performance of polymer microspheres. J. Mol. Liq. **308**, 113081 (2020)
17. J.P. Hooker, L. Delafresnaye, L. Barner, C. Barner-Kowollik, With polymer photoclicks to fluorescent microspheres. Mater. Horiz. **6**(2), 356–363 (2019)
18. T. Repenko, A. Rix, S. Ludwanowski, D. Go, F. Kiessling, W. Lederle et al., Bio-degradable highly fluorescent conjugated polymer nanoparticles for bio-medical imaging applications. Nat. Commun. **8**(1), 470 (2017)
19. Z. Hallaji, Z. Bagheri, B. Ranjbar, The role of fluorescent carbon dots in the fate of plastic waste. J. Environ. Chem. Eng.**110322** (2023)
20. D. Bartoš, M. Rewers, L. Wang, T.J. Sørensen, Incorporating fluorescent nanomaterials in organically modified sol–gel materials–creating single composite optical pH sensors. Sens. Diagnostics. **1**(1), 185–192 (2022)
21. L. Guo, L. Yang, M. Li, L. Kuang, Y. Song, L. Wang, Covalent organic frameworks for fluorescent sensing: recent developments and future challenges. Coord. Chem. Rev. **440**, 213957 (2021)
22. S. Khizar, N. Zine, A. Errachid, N. Jaffrezic-Renault, A. Elaissari, Microfluidic-based nanoparticle synthesis and their potential applications. Electrophoresis. **43**(7–8), 819–838 (2022)
23. G. Kibar, U. Çalışkan, E.Y. Erdem, B. Çetin, One-pot synthesis of organic–inorganic hybrid polyhedral oligomeric silsesquioxane microparticles in a double-zone temperature controlled microfluidic reactor. J. Polym. Sci., Part A: Polym. Chem. **57**(13), 1396–1403 (2019)
24. S. Orbay, A. Sanyal, Molecularly imprinted polymeric particles created using droplet-based microfluidics: Preparation and applications. Micromachines. **14**(4), 763 (2023)
25. G. Kibar, O.B. Şahinoğlu, B. Kılınçlı, E.Y. Erdem, B. Çetin, V.C. Özalp, Biosensor for ATP detection via aptamer-modified PDA@ POSS nanoparticles synthesized in a microfluidic reactor. Microchim. Acta. **191**(3), 153 (2024)
26. M.D. Aşık, M. Kaplan, B. Çetin, N. Sağlam, Synthesis of iron oxide core chitosan nanoparticles in a 3D printed microfluidic device. J. Nanopart. Res. **23**(3), 62 (2021)
27. M.T. Gokmen, W. Van Camp, P.J. Colver, S.A. Bon, F.E. Du Prez, Fabrication of porous clickable polymer beads and rods through generation of high internal phase emulsion (HIPE) droplets in a simple microfluidic device. Macromolecules. **42**(23), 9289–9294 (2009)
28. M. Grochowicz, P. Pączkowski, B. Gawdzik, Investigation of the thermal properties of glycidyl methacrylate–ethylene glycol dimethacrylate copolymeric microspheres modified by Diels–Alder reaction. J. Therm. Anal. Calorim. **133**, 499–508 (2018)
29. T. Kaufmann, M. Gökmen, C. Wendeln, M. Schneiders, S. Rinnen, H.F. Arlinghaus et al., Sandwich'microcontact printing as a mild route towards monodisperse janus particles with tailored bifunctionality. Adv. Mater. **23**(1), 79–83 (2011)
30. M. Ma, Q. Zhang, T. Xin, H. Zhang, W. Geng, J. Zhou, Preparation and characterization of structure-tailored magnetic fluorescent Fe 3 O 4/P (GMA–EGDMA–NVCz) core–shell microspheres. J. Mater. Sci. **48**, 5302–5308 (2013)
31. G. Kibar, D.Ö. Dinç, In-situ growth of Ag on mussel-inspired polydopamine@ poly (M-POSS) hybrid nanoparticles and their catalytic activity. J. Environ. Chem. Eng. **7**(5), 103435 (2019)

32. G. Kibar, Spherical shape poly (M-POSS) micro/nano hybrid latex particles: one-step synthesis and characterization. J. Appl. Polym. Sci. **137**(41), 49241 (2020)
33. M.S. Samuel, M. Ravikumar, J.A. John, E. Selvarajan, H. Patel, P.S. Chander et al., A review on green synthesis of nanoparticles and their diverse biomedical and environmental applications. Catalysts. **12**(5), 459 (2022)
34. M.E. rul Solmaz, Microfluidic bio-particle manipulation for biotechnology. Biochem. Eng. J.**15** (2014)
35. S. Zeinali, B. Cetin, S.N.B. Oliaei, Y. Karpat, Fabrication of continuous flow microfluidics device with 3D electrode structures for high throughput DEP applications using mechanical machining. Electrophoresis. **36**(13), 1432–1442 (2015)
36. R. Singh, S. Kumar, Effect of mixing on nanoparticle formation in micellar route. Chem. Eng. Sci. **61**(1), 192–204 (2006)
37. Van der S. Graaf, M. Steegmans, Van Der R. Sman, C. Schroën, R. Boom, Droplet formation in a T-shaped microchannel junction: a model system for membrane emulsification. Colloids Surf., a **266**(1–3), 106–116 (2005)
38. L. Jiang, X. Li, L. Liu, Q. Zhang, Cellular uptake mechanism and intracellular fate of hydrophobically modified pullulan nanoparticles. Int. J. Nanomed.1825–1834 (2013)
39. A. Reisch, A.S. Klymchenko, Fluorescent polymer nanoparticles based on dyes: seeking brighter tools for bioimaging. Small. **12**(15), 1968–1992 (2016)
40. G. Kibar, Effect of Crosslinking Agent on Mesoporous Spherical POSS hybrid particles: synthesis, characterization and Thermal Stability. J. Inorg. Organomet. Polym Mater.1–10 (2023)
41. G. Kibar, Epoxy Functional Porous POSS Microparticle Synthesis. Hacettepe J. Biology Chem. **50**(4), 359–366 (2022). https://doi.org/10.15671/hjbc.879777
42. G. Kibar, Epoxy Functional Porous POSS Microparticle Synthesis. Hacettepe J. Biology Chem.**50**(4):359–366
43. S. Delavari, S. Ziadzade, J.K. Rad, V. Hamrang, A.R. Mahdavian, Anticounterfeiting and photoluminescent cellulosic papers based on fluorescent acrylic copolymer nanoparticles containing coumarin. Carbohydr. Polym. **247**, 116756 (2020)
44. I.D. Vukoje, E.S. Džunuzović, V.V. Vodnik, S. Dimitrijević, S.P. Ahrenkiel, J.M. Nedeljković, Synthesis, characterization, and antimicrobial activity of poly (GMA-co-EGDMA) polymer decorated with silver nanoparticles. J. Mater. Sci. **49**, 6838–6844 (2014)
45. G. Kibar, A.E. Topal, A. Dana, A. Tuncel, Newly designed silver coated-magnetic, monodisperse polymeric microbeads as SERS substrate for low-level detection of Amoxicillin. J. Mol. Struct. **1119**, 133–138 (2016)
46. G. Kibar, A. Tuncel, Synthesis and characterization of monodisperse-porous, zwitterionic microbeads. Polym. Bull. **73**, 1939–1950 (2016)
47. G. Kibar, B. Sarıarslan, S. Doğanay, G. Yıldız, O.B. Usta, B. Çetin, Novel 3D-Printed microfluidic magnetic platform for Rapid DNA isolation. Anal. Chem. **96**(5), 1985–1992 (2024)
48. J.A. Champion, S. Mitragotri, Role of target geometry in phagocytosis. Proceedings of the National Academy of Sciences.103(13):4930-4 (2006)
49. P. Kolhar, A.C. Anselmo, V. Gupta, K. Pant, B. Prabhakarpandian, E. Ruoslahti et al., Using shape effects to target antibody-coated nanoparticles to lung and brain endothelium. Proceedings of the National Academy of Sciences.110(26):10753-8 (2013)
50. U. Hatipoğlu, B. Çetin, E. Yıldırım, A novel zero-dead-volume sample loading interface for microfluidic devices: flexible hydraulic reservoir (FHR). J. Micromech. Microeng. **28**(9), 097001 (2018)
51. A. Atay, A. Topuz, B. Sarıarslan, E. Yıldırım, J. Charmet, K. Couling et al., Flow rate-controlled pipetting for microfluidics: second-generation flexible hydraulic reservoir (FHRv2). Microfluid. Nanofluid. **25**, 1–10 (2021)